J Comput Aided Mol Des (2014) 28:89–97
DOI 10.1007/s10822-014-9732-4

Prospective virtual screening for novel p53–MDM2 inhibitors using ultrafast shape recognition

Sachin P. Patil · Pedro J. Ballester · Cassidy R. Kerezsi

Received: 6 November 2013 / Accepted: 11 February 2014 / Published online: 20 February 2014

Abstract The p53 protein, known as the guardian of genome, is mutated or deleted in approximately 50 % of human tumors. In the rest of the cancers, p53 is expressed in its wild-type form, but its function is inhibited by direct binding with the murine double minute 2 (MDM2) protein. Therefore, inhibition of the p53–MDM2 interaction, leading to the activation of tumor suppressor p53 protein presents a fundamentally novel therapeutic strategy against several types of cancers. The present study utilized ultrafast shape recognition (USR), a virtual screening technique based on ligand–receptor 3D shape complementarity, to screen DrugBank database for novel p53–MDM2 inhibitors. Specifically, using 3D shape of one of the most potent crystal ligands of MDM2, MI-63, as the query molecule, six compounds were identified as potential p53–MDM2 inhibitors. These six USR hits were then subjected to molecular modeling investigations through flexible receptor docking followed by comparative binding energy analysis. These studies suggested a potential role of the USR-selected molecules as p53–MDM2 inhibitors. This was further supported by experimental tests showing that the treatment of human colon tumor cells with the top USR hit, telmisartan, led to a dose-dependent cell growth inhibition in a p53-dependent manner. It is noteworthy that telmisartan has a long history of safe human use as an approved anti-hypertension drug and thus may present an immediate clinical potential as a cancer therapeutic. Furthermore, it could also serve as a structurally-novel lead molecule for the development of more potent, small-molecule p53–MDM2 inhibitors against variety of cancers. Importantly, the present study demonstrates that the adopted USR-based virtual screening protocol is a useful tool for hit identification in the domain of small molecule p53–MDM2 inhibitors.

Keywords Ultrafast shape recognition · Virtual screening · DrugBank database · p53 · MDM2 · Colon cancer cells

Introduction

The tumor suppressor p53, a powerful pro-apoptotic protein, is dysregulated in virtually all human tumor cells [1]. The p53 gene is deleted or mutated in around 50 % of the cancers, with around 29,575 distinct gene mutations recorded so far [2]. The remaining 50 % of cancers express p53 in its wild-type form, but its function is inhibited by interaction with the human murine double minute 2 (MDM2) protein, an oncogenic protein over-expressed by cancer cells [3, 4]. The MDM2 protein binds to the N-terminal trans-activation domain of p53 and thus inhibits its transcriptional activity [5]. Moreover, MDM2 binding targets p53 for proteasomal degradation through E3 ubiquitin ligase activity [6]. Therefore, disrupting the protein–

Electronic supplementary material The online version of this article (doi:10.1007/s10822-014-9732-4) contains supplementary material, which is available to authorized users.

S. P. Patil (✉)
NanoBio Laboratory, Department of Chemical Engineering, Widener University, Chester, PA 19013, USA
e-mail: spatil@widener.edu

P. J. Ballester
European Bioinformatics Institute, Wellcome Trust Genome Campus, Hinxton, Cambridge CB10 1SD, UK

C. R. Kerezsi
Department of Biomedical Engineering, Widener University, Chester, PA 19013, USA

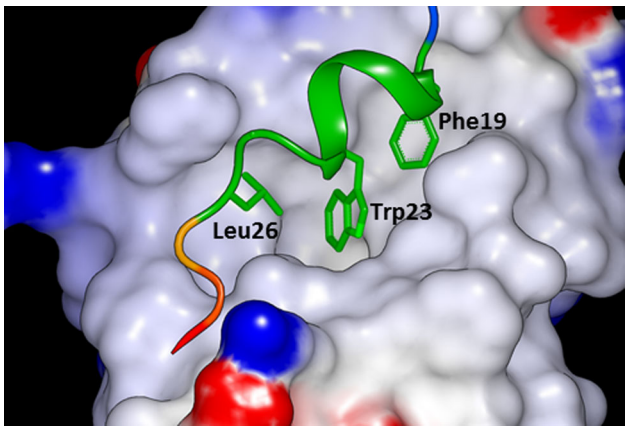

Fig. 1 Crystal structure of p53–MDM2 interaction (PDB: 1YCQ). Three key residues of p53 protein (Leu26, Trp23 and Phe19) are buried deep into a small, well-defined pocket on MDM2 protein, leading to the inhibition and proteasomal degradation of p53. The p53-binding pocket on MDM2 thus presents an important therapeutic target against cancer

protein interaction between p53 and MDM2 presents a fundamentally novel avenue for the treatment of variety of cancers. The published crystal structure of MDM2 bound with the p53 binding domain [7] has revealed three p53 residues (Leu26, Trp23 and Phe19) that are positioned deep into the binding cavity of MDM2 and thus are central to the binding (Fig. 1). Therefore, there is a significant interest in discovering small-molecule entities that can occlude this p53-binding cavity on MDM2 and in turn efficiently inhibit p53–MDM2 interaction. Such MDM2 inhibitors are expected to activate p53 protein and thus selectively induce cell cycle arrest, cellular apoptosis and tumor regression [8].

In this context, several different classes of inhibitors have been discovered that inhibited the p53–MDM2 interaction and proved the therapeutic promise of this novel strategy against variety of cancers. These inhibitors include low-molecular-weight compounds, small peptides, peptidomimetics and miniature proteins, with the small-molecule compounds being favored therapeutically due to their many advantages over other types of inhibitors [9]. The p53–MDM2 interaction has been shown to present a well-defined, small binding interface which has been proved to be highly amenable to the disruption using small molecules. Three of such most potent small-molecule MDM2 inhibitors include *cis*-imidazolines (Nutlins), spiro-oxindoles (MI series) and benzodiazepinedione analogs [8, 10–13]. These compounds mimic the three hydrophobic groups of p53 and thus target p53-binding pocket of MDM2 with high affinity. Here, it is noteworthy that compounds from spiro-oxindole and *cis*-imidazoline classes have recently progressed into the early clinical trials, but there is currently no approved drug targeting the p53–MDM2 interaction [14].

In the present study, 3D shape complementarity between MDM2 and its potent crystal ligand MI-63 was used to screen DrugBank database for potential p53–MDM2 inhibitors using Ultrafast Shape recognition (USR) technique. The USR-based virtual screening identified six molecules with high shape similarity with that of MI-63 and thus potentially similar biological activity. These USR hits were further subjected to flexible receptor docking and binding energy calculations to understand their probable binding modes with MDM2 and also to rank-order them in comparison with the native crystal ligand MI-63. The USR screening supported by induced-fit docking (IFD)and binding energy calculations revealed telmisartan, an approved anti-hypertension drug, as a potential p53–MDM2 inhibitor. Accordingly, telmisartan showed selective anti-proliferation activity in human colon tumor cell line expressing wild-type p53 (HCT116-p53$^{+/+}$) compared to corresponding isogenic p53-knockout cell line (HCT116-p53$^{-/-}$). Thus, telmisartan could serve as a promising drug candidate against several types of cancer expressing wild-type p53. Furthermore, these encouraging results also demonstrate that the USR-based screening protocol involving molecular shape complementarity can be a useful tool for screening other available databases for identification of potentially novel p53–MDM2 inhibitors.

Methods

Ligand-based virtual screening

The USR-based screening technique [15–17] was used to perform the ligand-based virtual screening of a molecular database, as it has demonstrated to be particularly successful in past prospective applications [18, 19]. The DrugBank database was extracted from ZINC online repository [20]. The database contained ~7,000 molecules, including FDA-approved drugs, experimental drugs and neutraceuticals. The 3D conformers were generated for these molecules using OMEGA v. 2.1 with default control parameters (OpenEye Scientific Software, Inc., http://www.eyesopen.com), which gave rise to about ~6 million unique 3D conformers. USR was used to search this 3D conformer database for similarly shaped molecules to the known p53–MDM2 inhibitor (MI-63). The crystal structure of MI-63 was obtained from the published crystal structure of MDM2 bound with MI-63 [protein data bank (PDB): 3LBL] [21]. The compounds were ranked by using USR similarity score of the highest ranking conformer of each compound. This led to six drug molecules with highest shape similarity to MI-63's co-crystallized pose (USR score

>0.90), which were subjected to further molecular modeling studies.

Induced-fit docking

Crystal structure of MDM2 (PDB: 3LBL) [21] downloaded from the PDB [22] was used for the molecular docking studies. The protein structure was prepared using the protein preparation wizard in the Schrodinger graphical user interface Maestro (version 9.5). Bond orders were assigned to the ligand in the crystal structure and hydrogen atoms were added to the protein–ligand complex consistent with the physiologic pH (7.0). The missing side chains and loops were filled using Prime (version 3.3). The X-ray water molecules were removed during protein preparation, which has been previously shown to be a reasonable assumption based on molecular dynamics studies [23]. The starting ligand conformations of the 6 USR hits were obtained by carrying out a Monte Carlo conformational search using Macromodel 10.1 (Schrödinger, LLC). Here, the OPLS_2005 force field was used for the conformational search with GB/SA continuum water solvation model, followed by the Polak-Ribiere Conjugate Gradient (PRCG) energy minimization of 5,000 steps or until the energy difference between subsequent structures reached 0.05 kJ/mol. The protein and ligand structures thus prepared were used for IFD as described below.

The IFD protocol was run with default parameters from the Maestro 9.5 graphical user interface. The first stage of IFD protocol involved use of Glide 4.0 (Schrödinger) to generate 80 initial poses through softened-potential docking step, enabling tolerance of more steric clashes as compared to a normal docking protocol. The second stage involved protein refinement using Prime 3.3 module to allow the active site conformational change around 5.0 Å of the initial poses, with energy minimization being carried out using OPLS_2005 force field and Prime's implicit solvent model. This active-site modification was followed by further refinement by prime and re-docking by Glide SP scoring function leading to the generation of the final IFD models. These IFD poses were graphically visualized using the Maestro 9.5 graphical user interface.

Energy minimization using eMBrAcE

To further investigate the association of the ligands with MDM2, the automated mechanism in the multi-ligand bimolecular association with energetics (eMBrAcE) module incorporated in MacroModel 10.1 was used. Specifically, the eMBrAcE module determined the binding energy differences through minimization using OPLS_2005 force field. All the calculations were performed with GB/SA continuum water solvation model. The extended cut-off value of 8.0 Å for vdW and 20.0 Å for electrostatic interactions were used to set up the force field. The minimization calculations were performed for 5,000 steps or until the energy difference between subsequent structures was 0.05 kJ/mol. The eMBrAcE calculations were carried out for each ligand–receptor complex in the "energy difference mode". This mode calculates the minimized energy of both the separate protein and ligand subtracted from the minimized energy of the whole protein–ligand complex to estimate the energy changes upon binding. Thus, eMBrAcE calculations in this mode provided total energy difference ($\Delta E_{Total} = E_{complex} - E_{ligand} - E_{protein}$) for each complex, which was used for the comparative binding energy study of USR hits with the native crystal MDM2 ligand, MI-63.

In-vitro cell proliferation study

The human colon tumor cell line expressing wild-type p53 (HCT116-p53$^{+/+}$) and the corresponding isogenic p53-null cell line (HCT116-p53$^{-/-}$) were grown in McCoy's 5A modified media (Invitrogen) supplemented with 10 % FBS (Invitrogen) in a humidified environment with 5 % CO_2 and 37 °C. The cells were plated in 96-well plates at the density of ~3,000 cells/well and treated with various concentrations of the top USR hit telmisartan and the known p53–MDM2 inhibitor Nutlin-3. First, the 10 mM stock solutions of both telmisartan and Nutlin-3 were prepared in DMSO and stored in aliquots at −20 °C. Then, the respective test concentrations of these compounds were prepared fresh in cell culture medium, adjusted to pH 7.4, sterilized with 0.22 μm filter and used for cell treatment. After 72 h of treatment, the effect on cell proliferation was evaluated by using the WST-1 cell proliferation assay (Millipore) as per the manufacturer's instructions.

Results and discussion

The present study involved use of 3D shape-based USR screening of the DrugBank database, followed by the structure-based docking studies and energy minimization calculations to rank-order the promising molecules for further experimental testing in HCT116 human tumor cell lines.

3D shape-based database screening using USR

Crystal structures of several different classes of small-molecule ligands in complex with MDM2 are currently available [24], which present the precise spatial and chemical requirements necessary for the effective binding of a given molecule to the p53-binding pocket on MDM2.

Table 1 3D shape scores and multi-ligand bimolecular association with energetics (eMBrAcE) calculations of MI-63 and 6 USR hit molecules

Molecules	3D USR score	2D MACCS score	Energy difference (ΔE: kJ/mol)
Query: MI-63	1.000	1.000	−150.0
ZINC01530886	0.918	0.467	−145.2
ZINC12504151	0.916	0.424	−158.3
ZINC12501050	0.912	0.416	−119.6
ZINC03872863	0.909	0.275	−107.6
ZINC03817099	0.905	0.580	−102.4
ZINC12502561	0.903	0.439	−87.3

Out of these, the MDM2 inhibitors from *cis*-imidazoline (e.g. Nutlins), spiro-oxindoles (e.g. MI series compounds) and benzodiazepinedione classes are the most promising ones with the spiro-oxindole ligand MI-63 being the most potent one [25]. Therefore, we first used the USR technique to search DrugBank database for drug molecules with high shape similarity to that of the MI-63 co-crystallized ligand (PDB: 3LBL). It is noteworthy that the ligand-centric, shape-based virtual screening has been suggested to obtain more consistent performance across targets in terms of hit rate than other 3D screening methods including structure-based docking and 3D pharmacophore screening [26]. More importantly, shape similarity techniques often lead to new inhibitors with innovative chemical scaffolds [18, 19]. In this regard, the USR screening of the DrugBank database revealed top 6 hits that contained approved and experimental drugs with 3D shape similarity score $\geq$0.90 (Table 1). The chemical structures of query molecule MI-63 and the 6 USR hits are shown in Fig. 2. These compounds show a good shape-similarity with the known ligand MI-63, but possess structurally novel scaffolds as compared to MI-63. This is further supported by the observed low 2D MACCS scores (Table 1) for majority of these molecules as compared to the query molecule (MI-63).

Induced-fit docking and binding energy studies of USR hits

The molecular modeling studies of USR hits with respect to the crystal ligand of MDM2 (MI-63) were carried out for investigating their binding modes with the p53-binding pocket on MDM2. As shown in Fig. 2 and Table 1 (2D MACCS scores), all of these compounds are structurally different and thus may not be expected to fit in the MDM2 pocket in the same way as that of the crystal ligand MI-63. Due to this, the IFD methodology was used for docking, as it has been shown previously to be effective in handling the receptor flexibility for structurally different ligands [27]. The binding modes of MI-63 and 6 USR hits, obtained through successful IFD followed by minimization, are shown (Fig. 3 and Supplementary Fig. S1). The conformation of MI-63 obtained through IFD shared a very similar binding mode as its reported crystal structure (PDB: 3LBL). Specifically, the Trp23 sub-pocket on MDM2 is correctly filled with 6-chlorooxindole ring of MI-63, which formed a hydrogen bond with the Leu54 residue of MDM2. Moreover, the 2-fluoro-3-chlorophenyl ring and the neopentyl group of MI-63 filled the remaining two MDM2 sub-pockets, Leu26 and Phe19, respectively. Similarly, the corresponding hydrophobic groups of the USR hits occupied the hydrophobic, p53-binding sub-pockets on MDM2. Specifically, top 5 out of 6 USR hits (ZINC IDs: 01530886, 12504151, 12501050, 03872863, 03817099) occupied three sub-pockets on MDM2 correctly. The last USR hit (ZINC12502561), on the other hand, occupied only two out of three MDM2 sub-pockets and thus may be a weak inhibitor of p53–MDM2 interaction. The ligand–protein interactions revealed important hydrophobic interactions of these ligands with key MDM2 residues (Gly58, ILE61, Leu54, Tyr67, Tyr100 and Val93). All of the ligands, except ZINC03872863, also formed at least one hydrogen bond with the MDM2 residues. These binding modes of USR hits are consistent with those of the known MDM2 crystal ligands including MI-63. Thus, clearly majority of USR hits have structural features to accommodate in the MDM2 pocket, which may lead to potential p53–MDM2 interaction inhibition. Furthermore, the eMBrAcE energy calculations are shown in Table 1 for USR hits in comparison to MI-63 for MDM2. As shown, the top 2 USR hits that are also predicted by IFD to correctly occupy three sub-pockets on MDM2 also showed favorable binding energies with MDM2 comparable to its native crystal ligand MI-63. Here, it is noteworthy that the rigid-receptor docking with AutoDock Vina also qualitatively ranked the USR hits in the same order as the eMBrAcE energy calculations (Supplementary Table S1). These data thus comply with the IFD studies and further justify possible activity of these USR-selected molecules as potential p53–MDM2 inhibitors. The RMSD values for IFD and AutoDock Vina docking poses of crystal ligand MI-63 were 1.810 and 0.405 Å, respectively. The relatively higher RMSD value for the IFD pose may be attributed to the observed rotation of 2-fluoro-3-chlorophenyl ring of MI-63 with the F and Cl atoms pointing outward of the MDM2 pocket (Fig. 3). Nevertheless, both IFD and AutoDock Vina proved well-suited for our docking studies, revealing several drug molecules that can occupy the p53-binding pocket on MDM2 well.

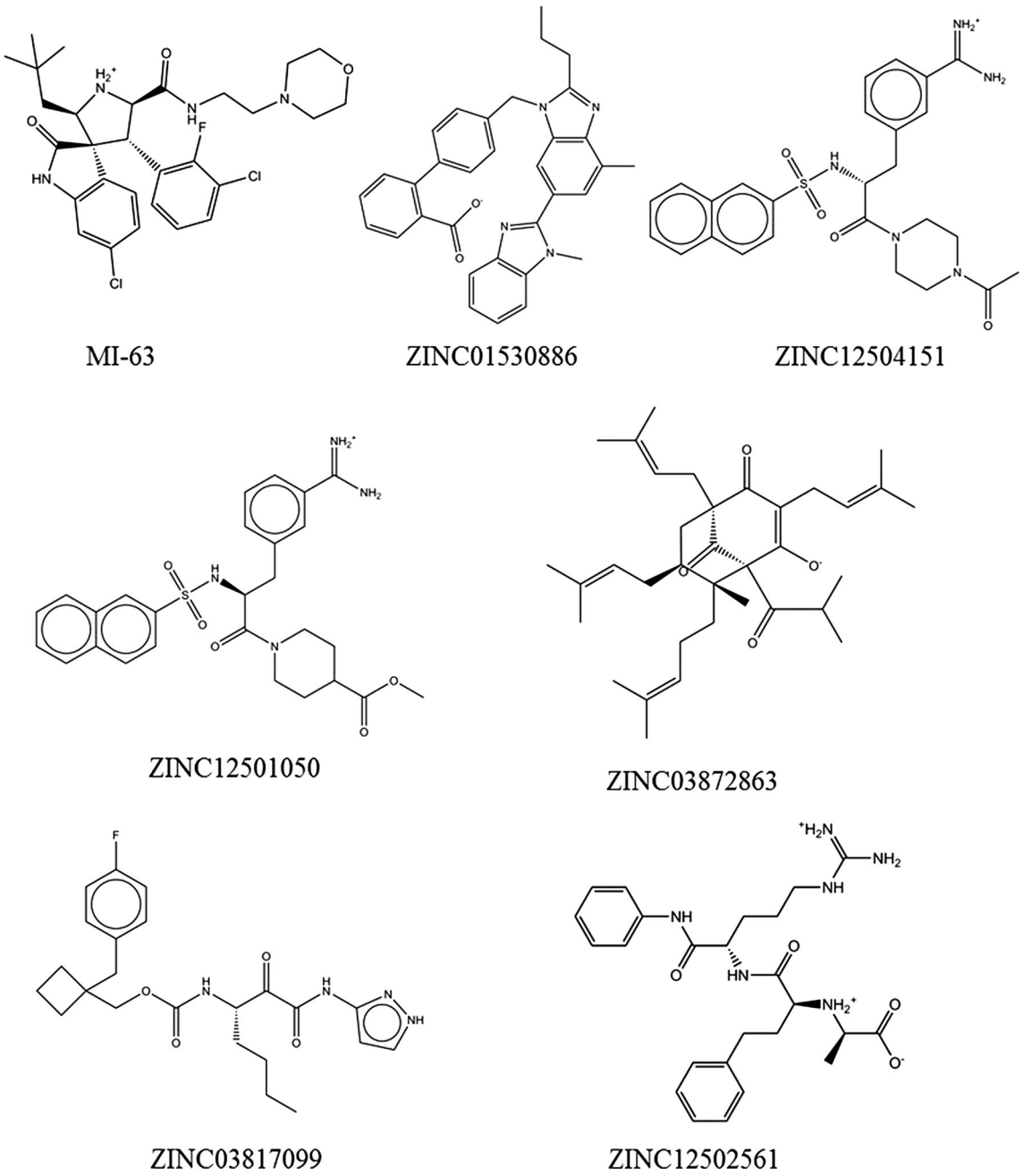

Fig. 2 Chemical structures of MDM2 crystal ligand MI-63 and 6 top hits obtained through USR-based screening of the DrugBank database

Cancer cell growth inhibition

The computational results indicated a potential disruptive role of USR hits in inhibiting p53–MDM2 interaction, which is expected to lead to p53 activation followed by selective growth inhibition in cancer cells expressing wild-type p53. In this context, experimental studies were carried out on one the top USR hit molecule (ZINC01530886), which is an approved anti-hypertension drug telmisartan. A well-characterized, small-molecule disruptor of p53–MDM2 interaction, Nutlin-3 was used as a positive control. Telmisartan, similar to Nutlin-3, was found to dose-dependently inhibit growth of HCT116-$p53^{+/+}$ cells, but had no effect on the growth of cells lacking p53 gene (HCT116-$p53^{-/-}$ cells) (Fig. 4). These novel experimental findings demonstrate that this approved anti-hypertension drug is a p53-dependent inhibitor of human colon cancer cell proliferation in vitro. Furthermore, telmisartan showed a broad spectrum, anti-proliferative activity in the NCI60 human tumor cell line screen, with lower average GI_{50}

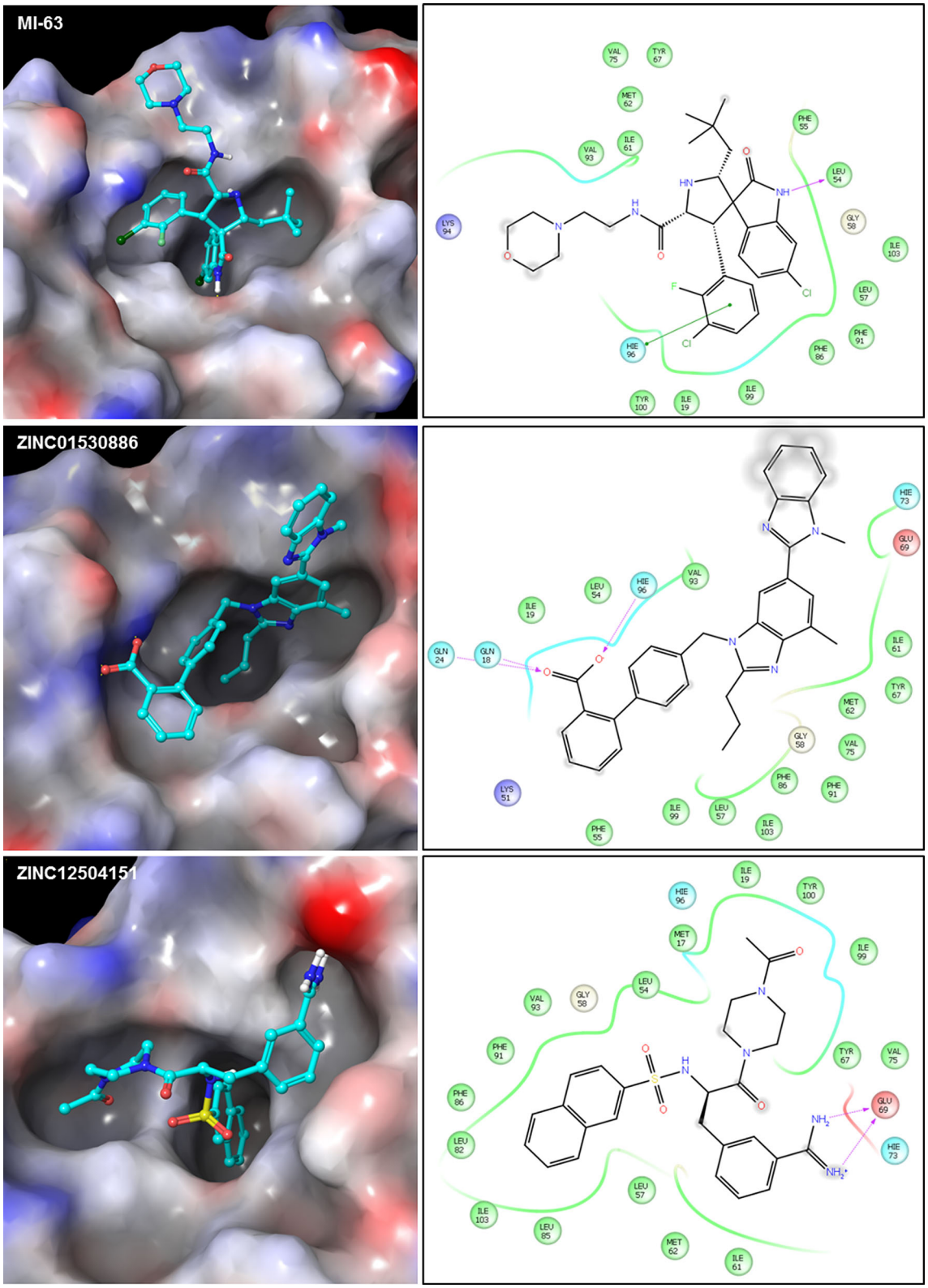

Fig. 3 The binding modes of MDM2 crystal ligand MI-63 and 2 of the top-ranking USR hits (ZINC01530886 and ZINC12504151) obtained through IFD followed by minimization. (*Left panel*) surface representation of p53-binding pocket on MDM2 containing bound ligands (*right panel*) 2D ligand–protein interaction diagrams

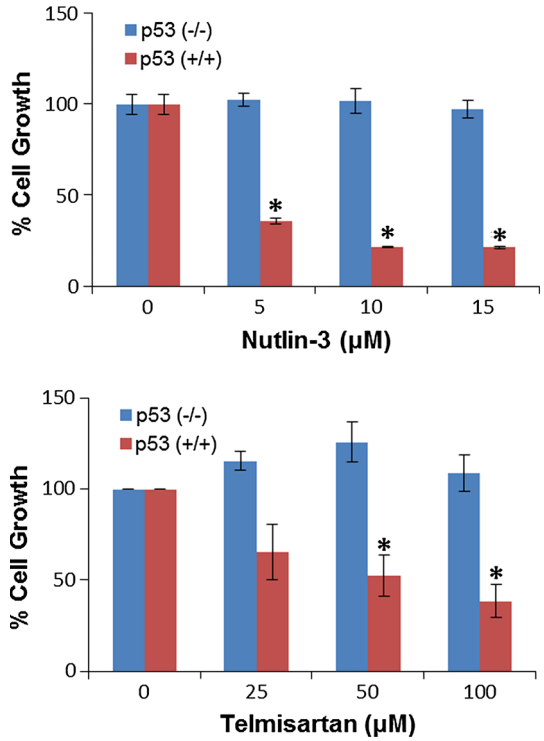

Fig. 4 WST-1 cell proliferation assay. The HCT116-p53$^{+/+}$ and -p53$^{-/-}$ cells were incubated for 72 h with Nutlin-3 (positive control) and telmisartan (top USR hit), both of which dose-dependently inhibited growth of p53$^{+/+}$ cells, while having a non-significant effect on p53$^{-/-}$ cell growth. Student's t test, $^{*}p < 0.05$ compared to control

value in wt-p53 cells as compared to cells expressing mutant-p53 (Supplementary Table S2 and Fig. S2). Thus our data, taken together with the presented computational analysis, may suggest that the observed whole-cell activity is potentially a result of telmisartan disrupting the p53–MDM2 interaction. We hope that the presented results will encourage X-ray crystallographers to investigate binding mode of telmisartan with MDM2, further establishing it as a novel p53–MDM2 inhibitor. The potential functional activity of other USR hits remains to be investigated.

Here, it should be noted that the observed cellular activity of telmisartan is significantly lower than the known p53–MDM2 inhibitor Nutlin-3 (Fig. 4). This may be attributed to the limited cellular uptake of telmisartan, possibly due to the presence of a carboxyl acid group in telmisartan structure [28]. This hypothesis is supported by a recent study that showed that ethyl ester of a previously discovered carboxylic acid MDM2 inhibitor (YH239) significantly increased its cellular activity as compared to the parent compound [29]. Furthermore, careful comparison of chemical structures of telmisartan and the known p53–MDM2 inhibitor MI-63 shows presence of three hydrophobic residues which are central for occupying three key hydrophobic pockets (Leu26, Trp23 and Phe19) on MDM2. In addition to these three hydrophobic residues, however, MI-63 contains a hydrophilic morpholine moiety, while telmisartan contains a hydrophobic benzodiazolyl moiety. Another benchmark p53–MDM2 inhibitor, Nutlin-3, also contains a hydrophilic 2-piperazinone moiety in addition to the three hydrophobic features. These key structural differences in terms of presence or absence of a hydrophilic residue may be responsible for the observed low-micromolar, whole-cell activity of telmisartan as opposed to the nanomolar activity of MI-63 and Nutlin-3 [10]. Here, it is noteworthy that the presence of a hydrophilic group is known to provide a protective cover for the hydrophobic binding interface from the surrounding solvent and thus significantly increase the MDM2 binding energy [24]. In this regard, telmisartan is highly hydrophobic, which may require structural optimization for enhanced MDM2 binding and p53 activation. For example, structural modification of telmisartan with a solvent-exposed hydrophilic moiety, in place of hydrophobic benzodiazolyl group or at other appropriate position, may have beneficial influence on the MDM2 binding. Such structural analogs of telmisartan, possibly also lacking the carboxyl group, may prove even more potent for MDM2 inhibition leading to enhanced p53 activation against variety of cancers. Despite having weaker whole-cell activity than the known p53–MDM2 inhibitors, telmisartan has the advantage of being safe as a drug and thus its use as a lead is attractive.

Conclusions

In the present study, USR-based virtual screening approach was applied to screen DrugBank database for potentially novel p53–MDM2 inhibitors. Several molecules were identified with 3D shapes similar to the known crystal ligand MI-63 and hence possibly having similar biological activity. The USR data were further supported by molecular modeling investigations involving IFD and binding energy calculations. Specifically, top USR hit telmisartan was suggested to bind to the p53-binding pocket on MDM2 and thus potentially leading to p53 activation. Accordingly, telmisartan showed p53-dependent cancer cell growth inhibition; growth inhibition observed in the HCT116 colon cancer cell line with wild-type p53, but not in the corresponding isogenic p53-null cell line. Previously, telmisartan has been shown to inhibit growth of prostate, renal and urological cancer cells [30–32], but was not active in lung cancer cell line expressing mutant p53 (Pubchem assay AID: 902). Taken together, these data further support a potential role of telmisartan in MDM2 inhibition followed by p53 activation leading to the

inhibition of cancer cell proliferation. The observed, anti-proliferation activity of telmisartan may be further enhanced through structural modification of telmisartan with solvent-exposed hydrophilic moieties that will protect telmisartan-MDM2 binding interface from solvent. As an approved anti-hypertension drug, telmisartan has a long history of safe use in humans and thus presents an immediate clinical potential as a cancer therapeutic. Furthermore, it could also serve as a structurally-novel "lead" molecule for the development of more potent, small-molecule p53–MDM2 inhibitors against variety of cancers expressing wild-type p53. Finally, these encouraging results demonstrate that the adopted USR-based virtual screening protocol can be a useful tool for identification of novel hits that can be developed into potent p53–MDM2 inhibitors for cancer therapy.

Acknowledgments We thank Dr. Bert Vogelstein at the Johns Hopkins University for the HCT-116 cell lines, Dr. Shirley Fischer-Drowos from the Department of Chemistry for her kind assistance with WST-1 assay and John Stoddart from the Department of Computer Science for his assistance with virtual database screening. We also thank the National cancer Institute (NCI) for carrying out NCI60 screening of telmisartan. The present study is supported by the Widener University Provost Grant to Dr. Sachin P. Patil and the Medical Research Council's Methodology Research Fellowship (Grant No. G0902106) to Dr. Pedro J. Ballester.

References

1. Harris SL, Levine AJ (2005) The p53 pathway: positive and negative feedback loops. Oncogene 24(17):2899–2908
2. Petitjean A, Mathe E, Kato S, Ishioka C, Tavtigian SV, Hainaut P, Olivier M (2007) Impact of mutant p53 functional properties on TP53 mutation patterns and tumor phenotype: lessons from recent developments in the IARC TP53 database. Hum Mutat 28(6):622–629
3. Chene P (2003) Inhibiting the p53–MDM2 interaction: an important target for cancer therapy. Nat Rev Cancer 3(2): 102–109
4. Momand J, Wu HH, Dasgupta G (2000) MDM2–master regulator of the p53 tumor suppressor protein. Gene 242(1–2):15–29
5. Toledo F, Wahl GM (2006) Regulating the p53 pathway: in vitro hypotheses, in vivo veritas. Nat Rev Cancer 6(12):909–923
6. Moll UM, Petrenko O (2003) The MDM2-p53 interaction. Mol Cancer Res 1(14):1001–1008
7. Kussie PH, Gorina S, Marechal V, Elenbaas B, Moreau J, Levine AJ, Pavletich NP (1996) Structure of the MDM2 oncoprotein bound to the p53 tumor suppressor transactivation domain. Science 274(5289):948–953
8. Vassilev LT, Vu BT, Graves B, Carvajal D, Podlaski F, Filipovic Z, Kong N, Kammlott U, Lukacs C, Klein C, Fotouhi N, Liu EA (2004) In vivo activation of the p53 pathway by small-molecule antagonists of MDM2. Science 303(5659):844–848
9. Zhan C, Lu W (2011) Peptide activators of the p53 tumor suppressor. Curr Pharm Des 17(6):603–609
10. Ding K, Lu Y, Nikolovska-Coleska Z, Wang G, Qiu S, Shangary S, Gao W, Qin D, Stuckey J, Krajewski K, Roller PP, Wang S (2006) Structure-based design of spiro-oxindoles as potent, specific small-molecule inhibitors of the MDM2-p53 interaction. J Med Chem 49(12):3432–3435
11. Grasberger BL, Lu T, Schubert C, Parks DJ, Carver TE, Koblish HK, Cummings MD, LaFrance LV, Milkiewicz KL, Calvo RR, Maguire D, Lattanze J, Franks CF, Zhao S, Ramachandren K, Bylebyl GR, Zhang M, Manthey CL, Petrella EC, Pantoliano MW, Deckman IC, Spurlino JC, Maroney AC, Tomczuk BE, Molloy CJ, Bone RF (2005) Discovery and cocrystal structure of benzodiazepinedione HDM2 antagonists that activate p53 in cells. J Med Chem 48(4):909–912
12. Shangary S, Qin D, McEachern D, Liu M, Miller RS, Qiu S, Nikolovska-Coleska Z, Ding K, Wang G, Chen J, Bernard D, Zhang J, Lu Y, Gu Q, Shah RB, Pienta KJ, Ling X, Kang S, Guo M, Sun Y, Yang D, Wang S (2008) Temporal activation of p53 by a specific MDM2 inhibitor is selectively toxic to tumors and leads to complete tumor growth inhibition. Proc Natl Acad Sci USA 105(10):3933–3938
13. Vassilev LT (2004) Small-molecule antagonists of p53–MDM2 binding: research tools and potential therapeutics. Cell Cycle 3(4):419–421
14. Warner WA, Sanchez R, Dawoodian A, Li E, Momand J (2012) Identification of FDA-approved drugs that computationally bind to MDM2. Chem Biol Drug Des 80(4):631–637
15. Ballester PJ (2011) Ultrafast shape recognition: method and applications. Future Med Chem 3(1):65–78
16. Ballester PJ, Finn PW, Richards WG (2009) Ultrafast shape recognition: evaluating a new ligand-based virtual screening technology. J Mol Gr Model 27(7):836–845
17. Ballester PJ, Richards WG (2007) Ultrafast shape recognition to search compound databases for similar molecular shapes. J Comput Chem 28(10):1711–1723
18. Ballester PJ, Mangold M, Howard NI, Robinson RL, Abell C, Blumberger J, Mitchell JB (2012) Hierarchical virtual screening for the discovery of new molecular scaffolds in antibacterial hit identification. J R Soc Interface 9(77):3196–3207
19. Ballester PJ, Westwood I, Laurieri N, Sim E, Richards WG (2010) Prospective virtual screening with ultrafast shape recognition: the identification of novel inhibitors of arylamine N-acetyltransferases. J R Soc Interface 7(43):335–342
20. Irwin JJ, Shoichet BK (2005) ZINC–a free database of commercially available compounds for virtual screening. J Chem Inf Model 45(1):177–182
21. Popowicz GM, Czarna A, Wolf S, Wang K, Wang W, Domling A, Holak TA (2010) Structures of low molecular weight inhibitors bound to MDMX and MDM2 reveal new approaches for p53–MDMX/MDM2 antagonist drug discovery. Cell Cycle 9(6):1104–1111
22. Berman HM, Westbrook J, Feng Z, Gilliland G, Bhat TN, Weissig H, Shindyalov IN, Bourne PE (2000) The protein data bank. Nucleic Acids Res 28(1):235–242
23. Wang F, Li Y, Ma Z, Wang X, Wang Y (2012) Structural determinants of benzodiazepinedione/peptide-based p53–HDM2 inhibitors using 3D-QSAR, docking and molecular dynamics. J Mol Model 18(1):295–306
24. Popowicz GM, Domling A, Holak TA (2011) The structure-based design of Mdm2/Mdmx-p53 inhibitors gets serious. Angew Chem 50(12):2680–2688
25. Joerger AC, Fersht AR (2010) The tumor suppressor p53: from structures to drug discovery. Cold Spring Harb Perspect Biol 2(6):a000919
26. Lee HS, Choi J, Kufareva I, Abagyan R, Filikov A, Yang Y, Yoon S (2008) Optimization of high throughput virtual screening by combining shape-matching and docking methods. J Chem Inf Model 48(3):489–497
27. Sherman W, Day T, Jacobson MP, Friesner RA, Farid R (2006) Novel procedure for modeling ligand/receptor induced fit effects. J Med Chem 49(2):534–553

28. Rothweiler U, Czarna A, Krajewski M, Ciombor J, Kalinski C, Khazak V, Ross G, Skobeleva N, Weber L, Holak TA (2008) Isoquinolin-1-one inhibitors of the MDM2-p53 interaction. ChemMedChem 3(7):1118–1128
29. Huang Y, Wolf S, Beck B, Kohler LM, Khoury K, Popowicz GM, Goda SK, Subklewe M, Twarda A, Holak TA, Domling A (2014) Discovery of highly potent p53–MDM2 antagonists and structural basis for anti-acute myeloid leukemia activities. ACS Chem Biol. doi:10.1021/cb400728e
30. Funao K, Matsuyama M, Kawahito Y, Sano H, Chargui J, Touraine JL, Nakatani T, Yoshimura R (2009) Telmisartan as a peroxisome proliferator-activated receptor-gamma ligand is a new target in the treatment of human renal cell carcinoma. Mol Med Rep 2(2):193–198
31. Matsuyama M, Funao K, Kuratsukuri K, Tanaka T, Kawahito Y, Sano H, Chargui J, Touraine JL, Yoshimura N, Yoshimura R (2010) Telmisartan inhibits human urological cancer cell growth through early apoptosis. Exp Ther Med 1(2):301–306
32. Takahashi S, Uemura H, Seeni A, Tang M, Komiya M, Long N, Ishiguro H, Kubota Y, Shirai T (2012) Therapeutic targeting of angiotensin II receptor type 1 to regulate androgen receptor in prostate cancer. Prostate 72(14):1559–1572